第32卷第10期 焊 接 学 报 Vol. 32 No. 10
2011年10月 TRANSACTIONS OF THE CHINA WELDING INSTITUTION October 2011

药芯焊丝焊接铝合金/不锈钢接头组织及性能分析

董红刚[1]， 杨丽群[1]， 翟 南[2]， 董 闯[3]
(1. 大连理工大学 材料科学与工程学院，大连 116085；2. 沈阳飞机工业有限公司，沈阳 110034；
3. 大连理工大学 三束教育部重点实验室，大连 116085)

摘 要：采用 ZnAl15 和 AlSi12 药芯焊丝成功实现了铝合金/不锈钢异种金属间的熔钎焊. 结果表明，焊态下采用 ZnAl15 药芯焊丝所得接头抗拉强度达 121 MPa；而 AlSi12 药芯焊丝所得接头抗拉强度最高可达 162 MPa. 接头经 280 ℃保温 30 min 焊后热处理后，采用 ZnAl15 药芯焊丝所得接头抗拉强度为 180 MPa，比焊态下接头抗拉强度高出将近一倍；采用 AlSi12 药芯焊丝所得接头强度可提高至 166 MPa. 对焊缝与钢之间的界面层进行成分分析发现，ZnAl15 药芯焊丝所得接头界面层主要由 Fe_2Al_5 和 $FeAl_3$ 等脆性化合物及锌固溶体组成，而 AlSi12 药芯焊丝所得接头界面层由 τ_5-$Al_{7.4}Fe_2Si$ 三元相组成，两种焊丝所得接头界面层厚度均不超过 10 μm.

关键词：铝合金；不锈钢；药芯焊丝；显微组织；力学性能
中图分类号：TG422.3 **文献标识码**：A **文章编号**：0253-360X(2011)10-0001-04

董红刚

0 序 言

铝及铝合金因比重轻、塑性好、耐腐蚀性强等特点在各种加工制造领域受到了越来越广泛的关注[1,2]；而钢作为一种最普通、应用最广的黑色金属，在制造业中的主导地位无法撼动，因此铝及铝合金与钢异种金属间的连接技术便成为亟需解决的问题[3,4].

由于铝合金在钢母材表面的润湿性较差，因此铝/钢异种金属连接过程中通常在钢表面镀锌等金属或涂敷钎剂以改善熔池金属在钢表面的铺展性能. 但该操作过程增加了生产工序和成本，影响了焊接过程的生产效率. Murakami 等人[5]采用 4047 药芯焊丝实现了纯铝板和低碳钢板异种金属间的直接弧焊连接，焊丝中的药芯改善了熔池金属在钢表面的润湿性，使得二者之间形成致密结合，所得接头的抗拉强度可达到铝合金母材的 70%. 林三宝等人[6]也采用 4047 药芯焊丝实现了铝合金和不锈钢板之间的弧焊连接，熔池金属在不锈钢表面铺展良好，润湿角不超过 30°，但在界面层中生成了大量脆性金属间化合物，恶化了接头性能，使得接头抗剪强度仅为 55 MPa.

收稿日期：2011-04-03
基金项目：国家自然科学基金资助项目(50904012/E041607)；辽宁省自然科学基金资助项目(20092152)

在以往的研究中，锌基实芯焊丝用于焊接铝/镀锌钢异种金属显示了优于铝基实芯焊丝的性能[7]，文中旨在研究锌基和铝基药芯焊丝对铝/无镀层钢接头微观组织和力学性能的影响，以期实现铝和无镀层钢异种金属间的高强连接.

1 试验方法

试验所用材料为厚 2 mm 的 5A02 铝合金板和厚 1.5 mm 的 AISI 304 不锈钢板，试件尺寸为 200 mm × 80 mm. 试验所用焊丝为直径 1.8 mm 的 ZnAl15 药芯焊丝和 AlSi12 药芯焊丝，药芯成分分别为 CsAlF4 和 KAlF4.

焊前用不锈钢丝刷清除母材表面(包括侧面)氧化膜，然后用丙酮擦拭待焊工件表面以去除油脂等污物. 焊接方法为交流 TIG 焊，接头形式采用搭接接头，搭接宽度为 18 mm. 为方便送丝，电弧长度保持在 5 mm. 保护气为氩气，气体流量为 10 L/min. 焊后，将接头进行大气气氛下 280 ℃保温 30 min 热处理，以对比研究焊后热处理对铝/钢接头微观组织及力学性能的影响. 采用两种药芯焊丝所用焊接工艺参数如表 1 所示.

将焊接接头制备成宽 25 mm 的拉伸试样，进行常温拉伸性能测试. 同时将典型焊件沿垂直焊接方向取样，制备焊缝金相试样，采用混合酸溶液(4 mL 氢氟酸 + 40 mL 硝酸 + 360 mL 去离子水)进行腐

表 1 焊接工艺参数及接头抗拉强度

Table 1 Welding parameters and tensile strength of Al/steel joints

样品编号	焊丝	焊接电流 I/A	行走速度 v_x/(mm·min^{-1})	送丝速度 v_s/(mm·s^{-1})	接头状态	抗拉强度 R_m/MPa
1	ZnAl15 药芯焊丝	40	60	3.5	焊态	89
2		40	60	3.5	热处理	180
3		50	120	4.5	焊态	121
4		50	120	4.5	热处理	143
5	AlSi12 药芯焊丝	40	60	5.3	焊态	162
6		40	60	5.5	热处理	141
7		50	60	7.4	焊态	162
8		50	60	7.4	热处理	166

蚀,使用光学显微镜(OM)和电子探针(EPMA)进行微观组织观察和成分分析.

2 试验结果及讨论

2.1 拉伸性能

采用 ZnAl15 药芯焊丝和 AlSi12 药芯焊丝所得接头抗拉强度如表 1 所示. 由表 1 可见,焊态下,采用 ZnAl15 药芯焊丝所得接头抗拉强度可达 121 MPa,而采用 AlSi12 药芯焊丝所得接头抗拉强度最高可达 162 MPa. 要获得高质量的铝/钢异种金属接头,采用 AlSi12 药芯焊丝焊接需要比 ZnAl15 药芯焊丝更高的焊接热输入,这是由于 AlSi12 药芯焊丝的熔点高于 ZnAl15 药芯焊丝. 对比焊态和退火后接头的抗拉强度可发现,焊后热处理能明显提高接头抗拉强度. 采用 ZnAl15 药芯焊丝所得接头经 280 ℃保温 30 min 退火处理后,抗拉强度由 89 MPa 提高至 180 MPa;而采用 AlSi12 药芯焊丝所得接头经退火处理后其强度达到 166 MPa. 焊态下,ZnAl15 药芯焊丝连接接头断裂于界面层处,退火处理后,接头强度增加,断裂发生在焊缝或铝母材侧. 而采用 AlSi12 药芯焊丝所得接头在焊态和退火态均沿焊缝断裂.

2.2 显微组织

采用 ZnAl15 药芯焊丝所得接头微观组织见图 1. 可以看出,焊缝组织主要由锌溶于铝中形成的富铝固溶体(Al)、铝溶于锌中形成的富锌固溶体(Zn)以及富锌氧化物组成,金属基体和氧化物陶瓷一起构成了金属陶瓷组织[8],该组织结合了金属材料的高韧性及陶瓷材料的高强度. 空气、水蒸气及焊接母材表面残存的氧化物使得氧成为焊接过程中不可避免的元素. 相关资料表明,焊缝中氧含量增加,其强度、硬度和塑性等性能会明显下降,甚至会引起金属的热脆、冷脆,恶化焊接接头的性能. 但试验中氧与锌结合形成了氧化物陶瓷相,对焊缝起到增强作用,获得了强度较高的焊接接头. 对比退火前后的焊缝组织可发现,退火后富锌氧化物分布更加弥散均匀,且呈网状,使得增强效果更好,接头抗拉强度更高. 图 2 为采用 AlSi12 药芯焊丝所得接头微观组织形貌,可见焊缝主要由 α-Al 和网状 Al-Si 共晶组织组成. 对比退火前后的微观组织可以发现,退火后焊缝区晶粒更为细小,由于退火温度较低,晶粒并未出现粗化,由细晶强化原理可知,焊缝区晶粒尺寸的减小可有效改善接头性能.

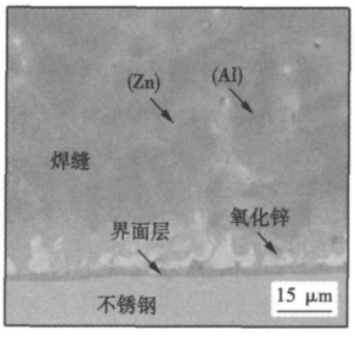

(a) 1号样品焊态接头

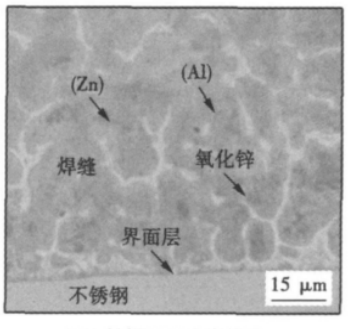

(b) 2号样品退火态接头

图 1 采用 ZnAl15 药芯焊丝所得接头微观组织形貌

Fig. 1 Microstructure of joints made with ZnAl15 wire

2.3 成分分析

图 3 给出了采用 AlSi12 药芯焊丝所得接头的

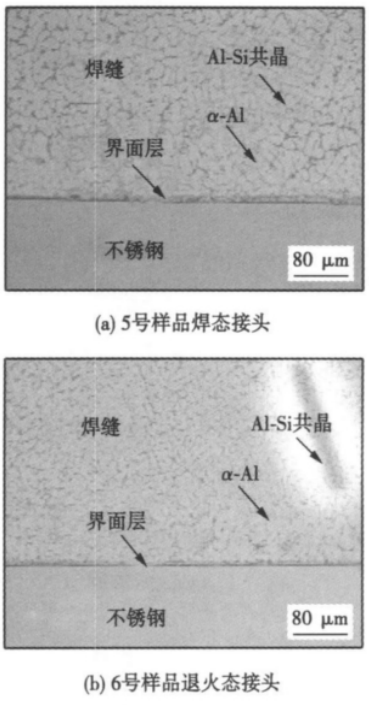

图 2　采用 AlSi12 药芯焊丝所得接头微观组织形貌

Fig. 2　Microstructure of joints made with AlSi12 wire

EPMA 面扫描结果. 由图 3 可见，AlSi12 药芯焊丝所得接头焊缝区域主要由 α-Al 组成，定量测试结果表明，该相中 Al 元素含量(质量分数，%)高达 98% ~ 99%，其中弥散分布 Al-Si 共晶组织. Fe 元素分析结果表明，尽管铝/钢连接过程中不锈钢母材并未熔化，但铁仍然扩散到焊缝与钢连接的界面层中，少部分铁甚至扩散进焊缝组织中形成少量富铁相.

铝/钢异种金属连接过程中，焊缝与钢连接处的界面层是影响接头性能的关键因素之一. 由图 1 可见，ZnAl15 药芯焊丝所得接头界面层比较均匀，其厚度不超过 1.5 μm，XRD 和 EPMA 分析结果表明该界面层主要由 Fe_2Al_5 和 $FeAl_3$ 等脆性 Fe-Al 金属间化合物及锌固溶体组成[8]. 而 AlSi12 药芯焊丝所得接头界面层厚度参差不齐，最薄区域厚度约为 1.6 μm，而最厚区域高达 8.6 μm. 成分分析表明界面层中 Al 元素的含量为 56.6% ~ 57.2%，Fe 元素的含量为 34.7% ~ 35.6%，Si 元素的含量为 7.2% ~ 8.6%. 焊丝中 Si 元素与不锈钢母材中 Fe 元素之间具有较高的亲和性，其通过形成 Al-Fe-Si 三元金属间化合物有效抑制 Fe-Al 脆性金属间化合物的产生. 由 Al-Fe-Si 三元相图可知，Al，Fe 和 Si 三种元素之间能形成 10 多种三元化合物，结合成分分析可知，该界面层中三元化合物主要为 τ_5-$Al_{7.4}Fe_2Si$ 相.

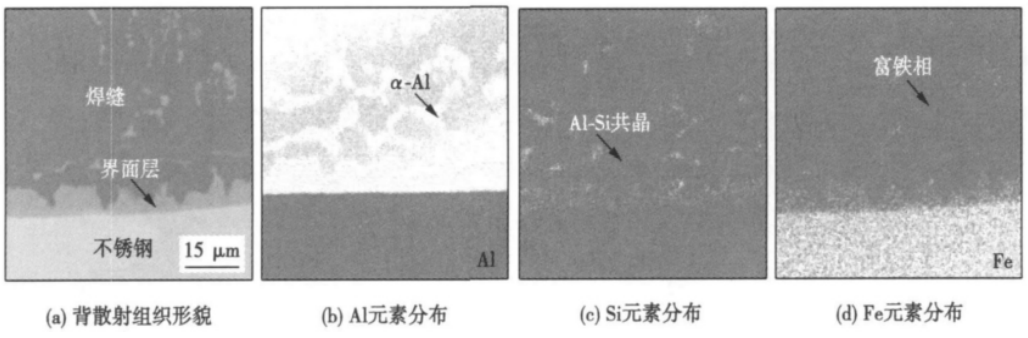

图 3　AlSi12 药芯焊丝所得接头 EPMA 面扫描结果

Fig. 3　EPMA map scanning results of joint sample No. 5 made with AlSi12 wire

3　结　　论

(1) 采用 ZnAl15 和 AlSi12 药芯焊丝均能实现铝合金/不锈钢异种金属间的良好连接，经大气气氛下 280 ℃保温 30 min 焊后热处理后，ZnAl15 药芯焊丝所得接头抗拉强度可达 180 MPa; 采用 AlSi12 药芯焊丝，焊态和退火处理后的接头抗拉强度均能达到 160 MPa.

(2) 采用 ZnAl15 药芯焊丝所得接头焊缝组织主要由富锌固溶体(Zn)、富铝固溶体(Al)和富锌氧化物组成，富锌氧化物的存在改善了接头力学性能; 采用 AlSi12 药芯焊丝所得接头焊缝则由 α-Al 固溶体和 Al-Si 共晶组织组成.

(3) 采用 ZnAl15 药芯焊丝所得铝/钢接头界面层厚度不超过 1.5 μm; 而 AlSi12 药芯焊丝中 Si 元素有效阻止了 Fe-Al 脆性金属间化合物的产生，界面层处主要生成 τ_5-$Al_{7.4}Fe_2Si$ 三元化合物，其呈锯齿状生长，使得界面层厚度参差不齐.

参考文献:

[1]　Miller W S, Zhuang L, Bottema J, *et al*. Recent development in

aluminium alloys for the automotive industry [J]. Materials Science and Engineering A, 2000, 280(1): 37 - 49.

[2] 李 军, 陈云霞, 李中兵. 汽车轻量化应用技术探讨 [J]. 汽车工艺与材料, 2010, 2: 12 - 17.
Li Jun, Chen Yunxia, Li Zhongbing. Research on the application of automotive lightweight [J]. Automobile Technology & Material, 2010, 2: 12 - 17.

[3] Taban E, Gould J E, Lippold J C. Dissimilar friction welding of 6061-T6 aluminum and AISI 1018 steel: properties and microstructural characterization [J]. Materials and Design, 2010, 31(5): 2305 - 2311.

[4] Sierra G, Peyre P, Deschaux-Beaume F, *et al*. Steel to aluminium key-hole laser welding [J]. Materials Science and Engineering A, 2007, 447(1/2): 197 - 208.

[5] Murakami T, Nakata K, Tong H, *et al*. Dissimilar metal joining of aluminum to steel by MIG arc brazing using flux cored wire [J]. ISIJ International, 2003, 43(10): 1596 - 1602.

[6] 林三宝, 宋建岭, 马广超, 等. 铝合金与不锈钢异种金属铝硅药芯焊丝TIG熔钎焊接头组织及性能 [J]. 焊接学报, 2009, 30(7): 9 - 12.
Lin Sanbao, Song Jianling, Ma Guangchao, *et al*. Microstructure and properties of dissimilar metals TIG welding-brazing joint of aluminum alloy to stainless using Al-Si flux-cored wire [J]. Transactions of the China Welding Institution, 2009, 30(7): 9 - 12.

[7] Staubach M, Juttner S, Fussel U. Joining of steel-aluminium mixed joints with energy-reduced GMA processes and filler materials on an aluminium and zinc basis [J]. Welding and Cutting, 2008, 7(1): 30 - 38.

[8] Dong H G, Yang L Q, Dong C, *et al*. Arc joining of aluminum alloy to stainless steel with flux-cored Zn-based filler metal [J]. Materials Science and Engineering A, 2010, 527(26): 7151 - 7154.

作者简介: 董红刚, 男, 1975年出生, 博士, 副教授. 主要研究方向为异种金属的连接、焊接工艺、焊接冶金、焊接热过程数值模拟等. 发表论文40余篇. Email: donghg@dlut.edu.cn

公 告

关于变更《焊接学报》采编平台网址的公告

根据焊接学报编辑部工作的需要, 原采编平台网址: www.hjxb.cb.cnki.net 现已停用, 现将采用新的采编平台网址: magazines.hwi.com.cn. 请论文作者、审稿专家和读者按新的采编平台网址登录. 论文作者投稿时, 应将其论文电子版发到《焊接学报》采编平台上, 还须将论文打印稿(纸质)一式两份寄到本刊编辑部. 这两项工作要求同时进行, 以便编辑部及时登记送审, 望周知.

焊接学报编辑部

2011年9月25日

MAIN TOPICS, ABSTRACTS & KEY WORDS

Analysis on microstructure and mechanical properties of aluminum alloy/stainless steel joint made with flux-cored filler metal DONG Honggang[1], YANG Liqun[1], ZHAI Nan[2], DONG Chuang[3] (1. Department of Materials Processing Engineering, Dalian University of Technology, Dalian 116085, China; 2. Shenyang Aircraft Industry Corporation LTD, Shenyang 110034, China; 3. Key Laboratory of Materials Modification, Ministry of Education, Dalian University of Technology, Dalian 116085, China). p 1 - 4

Abstract: Dissimilar metal joining between 5A02 aluminum alloy and AISI 304 stainless steel was conducted by gas tungsten arc welding with ZnAl15 and AlSi12 flux-cored filler metals, and the effect of the filler metal composition on the microstructures and mechanical properties of the joints were investigated. The results revealed that the tensile strength of as-welded joints made with ZnAl15 and AlSi12 flux-cored filler metals was 121 MPa and 162 MPa respectively. After annealed at 280 ℃ for 30 min, the tensile strength of joints made with ZnAl15 flux-cored filler metal reached 180 MPa, while that with AlSi12 flux-cored filler metal was 166 MPa. The interfacial layer in the weld made with ZnAl15 filler metal was comprised of [$FeAl_3$] Zn_x and [Fe_2Al_5] Zn_x, and ternary intermetallic compound $Al_{7.4}Fe_2Si$ was found in the interfacial layer in the joint made with AlSi12 flux-cored filler metal. The thickness of the interfacial layers made with both filler metal was less than 10 μm.

Key words: aluminum alloy; stainless steel; flux-cored filler metal; microstructure; mechanical properties

Analysis on electromagnetic heat strengthening of welded joint with embedding crack and mechanical performance testing ZHENG Lijuan, CHAI Xuan, HAN Xiaojuan, FU Yuming (School of Mechanical Engineering, Yanshan University, Qinhuangdao 066004, China). p 5 - 8

Abstract: Numerical simulation on welded joint of 45 steel using electromagnetic heating was made by ANSYS. The temperature and residual stress field were analysed. The result showed that the crack tip in the welded joint melted and dulled after discharge, the stress concentration also was reduced, in addition, the three residual compressive stress field around welded crack tip was appeared. The tensile properities were tested to compare the mechanical performance before and after pulsed current discharges. The result indicated that tensile strength and elongation were improved. Numerical analysis and experimental research confirmed the feasibility of applying electromagnetic heat strengthening technology into welding field.

Key words: welded joint; embedding crack; electromagnetic heat strengthening; numerical analysis; mechanical properties

Numerical simulation and experimental test of DP590 dual-phase steel welding LI Huiqin, LIU Yixuan, HAN Qiang, MA Yonglin (School of Material and Metallurgy, Inner Mongolia University of Science & Technology, Baotou 014010, China). p 9 - 12

Abstract: DP590 dual-phase steel weld temperature field was analyzed by using ANSYS softwere. A program was developed with APDL language supported by the ANSYS, combining the body heat rate and element birth and death technology to simulate the welding filling process and heat input. A butt welding experiment with the DP590 dual-phase steel (3.8 mm thickness) was done in order to verify the accuracy of the simulation calculation. It is verified that numerical simulation is feasible.

Key words: DP590 dual-phase steel; numerical simulation; temperature field

Effects of laser shock processing on H_2S stress corrosion fractures of X70 pipeline steel welded joints KONG Dejun, WU Yongzhong, LONG Dan (College of Mechanical & Energy Engineering, Jiangsu Polytechnic University, Changzhou 213016, China). p 13 - 16

Abstract: The surfaces of X70 pipeline steel welded joints were processed with laser shock and its stress corrosion sensitivity was investigated in NACE saturated H_2S solutions by slow strain rate testing (SSRT). The fracture surfaces were analyzed with scanning electric microscope (SEM). The results show that the X70 pipeline steel welded joints in primitive state is brittle fracture. The cracks of tensile fracture is stress corrosion cracking. The mechanical properties of the X70 pipeline steel welded joints after laser shock processing is enhanced, its dimple dimension and depth becomes smaller, and the fracture mode is ductile fracture. SCC is the main mechanism of X70 pipeline steel welded joint stress corrosion cracking. Laser shock processing reduces the tendency of SCC and improves stress corrosion resistance H_2S of the welded joint.

Key words: X70 pipeline steel; welded joint; laser shock processing; stress corrosion

Analysis on corrosion behavior of welded joint of A7N01S-T5 aluminum alloy for high-speed train GOU Guoqing[1], HUANG Nan[1], CHEN Hui[1], LI Da[1], MENG Lichun[2] (1. College of Materials Science and Technology, Southwest Jiaotong University, Chengdu 610031, China; 2. CSR Qingdao Sifang Co., Ltd., Qingdao 266111, China). p 17 - 20

Abstract: Salt fog corrosion tests were employed to observe the corrosion behavior of welded joint of A7N01S-T5 aluminum alloy for high-speed train. The results showed that many corrosion products and pits distributed on the surface of the wel-